THE JOURNAL OF PHYSICAL CHEMISTRY B

Article

pubs.acs.org/JPCB

Supramolecular Interaction between a Hydrophilic Coumarin Dye and Macrocyclic Hosts: Spectroscopic and Calorimetric Study

Aninda Chatterjee, Banibrata Maity, and Debabrata Seth*

Department of Chemistry, Indian Institute of Technology Patna, Patna 800013, Bihar, India

Supporting Information

ABSTRACT: The photophysics of a hydrophilic molecule, 7-(diethylamino)-coumarin-3-carboxylic acid (7-DCCA), was studied in the presence of two macrocycles, (2-hydroxypropyl)-γ-cyclodextrin and cucurbit[7]uril. We have used steady-state absorption, fluorescence, and time-resolved fluorescence emission spectroscopy; Fourier transform infrared (FTIR) spectroscopy; ^{1}H NMR spectroscopy; and isothermal titration calorimetry (ITC) to confirm the supramolecular host−guest complex formation. The spectral properties of 7-DCCA were modulated in the presence of both macrocycles. It was assigned that 7-DCCA forms a 1:2 complex with (2-hydroxypropyl)-γ-cyclodextrin and cucurbit[7]uril. The large modulation of the emission properties of 7-DCCA in the presence of the macrocycles indicates the formation of supramolecular complexes. A significant shift in the bond vibration frequencies in the FTIR studies showed encapsulation of the dyes in the hydrophobic cavity of the macrocycles. This is further substantiated by the ^{1}H NMR studies, in which the upfield and downfield shifts of the protons were observed in both the aliphatic and aromatic region in the presence of macrocycles. The time-resolved anisotropy measurements further reinforce the conception of host−guest supramolecular complex formation because, in both cases, the rotational relaxation time increases significantly compared to that in water. A deeper understanding between the differences in interaction of an anionic molecule with cucurbit[7]uril and (2-hydroxypropyl)-γ-cyclodextrin will be achieved through this work. From the ITC measurement, we have formulated the forces due to complex formation.

1. INTRODUCTION

Supramolecular hosts and molecular containers are excellent media for providing the photostabilization of different photosensitive molecules and provide stabilization of different guest molecules by protecting them from the outside environment. Host−guest complexation is the simplest and most convenient process for tuning the molecular properties of guest molecules in a desired way by stimuli responsive and reversible noncovalent interaction.[1,2] Among different kinds of supramolecular macrocyclic hosts, the most important are cyclodextrins, calixarenes, and cucurbit[*n*]urils. For a long time, the host−guest complexation has been used for modulating the guest molecular properties.[3,4] For these purposes, several supramolecular assemblies such as cyclodextrins, cucurbit[*n*]urils, calix[*n*]arenes, etc. have been used as the host.[5−7] These macrocycles provide an environment more hydrophobic than the bulk solution by forming the inclusion or encapsulation complexes with the guest molecules and modulate the emission behavior of guest molecules. The journey of cucurbit[*n*]urils started in 1905, when the precursor of cucurbit[*n*]urils by the condensation reaction between the glycoluril and formaldehyde was first reported by Robert Behrend and co-workers.[8] They accidentally prepared a mysterious white colored solid, which was soluble in water in the presence of either protons or alkali ions, but could not recognize the compound to be the precursor of future supramolecular macrocycle cucurbit[*n*]urils. However, that discovery opened a new era.[9] Seventy-five years after this discovery, Freeman et al. studied extensively the structure of the previously discovered white solid and concluded that the solid was a pumpkin-shaped macrocyclic hexamer and named it after the biological name of pumpkin, "cucurbituril".[10] Since then, cucurbit[*n*]urils have been used extensively for studying host−guest complexation. Because they are biologically relevant for their low in vivo and in vitro toxicity,[11] they have attracted significant attention of modern day researchers. Several researchers have studied the host−guest complexation using cucurbit[7]uril (CB7) as host molecule.[12−26] Beside this unique supramolecular macrocyclic host CB7, we have used 2-hydroxypropyl-γ-cyclodextrin (HP-γ-CD) as a host molecule to study host−guest dynamics. We have used HP-γ-CD because it has greater solubility in water compared to that of γ-cyclodextrin and greater binding affinity.[27] Previously, host−guest complexation in HP-γ-CD has been studied in very few cases.[28] The coumarin dyes with 7-monoalkyl and dialkylamino substitution are used as excellent fluorescent probes for observing the different, interesting photophyscial aspects.[29−38] The photophysical properties of these substituted amino coumarin dyes depend on the nature of the surrounding medium. In polar solvents, the excited state of these amino coumarin dyes are deactivated by intramolecular

Received: March 25, 2014
Revised: July 20, 2014
Published: July 21, 2014

dx.doi.org/10.1021/jp502944h | J. Phys. Chem. B 2014, 118, 9768−9781

Table 1. Photophysical Parameters of 7-DCCA (~3 × 10^{-6} M) in the Presence of HP-γ-CD and CB7

sr no.	system	λ_{abs} (nm)	λ_{emi} (nm)	ϕ_f	k_r (s^{-1})	k_{nr} (s^{-1})
1	7-DCCA in water	409	472	0.03	2.14 × 10^8	6.93 × 10^9
2	7-DCCA in water +1.35 mM HP-γ-CD	406	466	0.043	1.81 × 10^8	4.04 × 10^9
3	7-DCCA in water + 3.75 mM HP-γ-CD	405	463	0.051	1.51 × 10^8	2.81 × 10^9
4	7-DCCA in water + 6.93 mM HP-γ-CD	403	461	0.061	1.38 × 10^8	2.12 × 10^9
5	7-DCCA in water + 1.20 × 10^{-6} M CB7	408	473	0.036	1.71 × 10^8	4.59 × 10^9
6	7-DCCA in water + 5.37 × 10^{-6} M CB7	414	474	0.112	1.47 × 10^8	1.16 × 10^9
7	7-DCCA in water + 1.01 × 10^{-5} M CB7	418	474	0.161	1.53 × 10^8	7.99 × 10^8
8	7-DCCA in water + 2.00 × 10^{-5} M CB7	421	474	0.206	1.50 × 10^8	5.80 × 10^8

charge transfer (ICT). Sometimes it follows ultrafast twisting to produce a highly polar twisted intramolecular charge transfer (TICT) state.[39−42] In the presence of a host molecule the emission properties of coumarin were modulated because of the formation of a host−guest complex.

In this work, we have studied the supramolecular host−guest photodynamics between a hydrophilic molecule, 7-(diethylamino)-coumarin-3-carboxylic acid (7-DCCA), in the presence of two macrocycles, CB7 and HP-γ-CD. We had seen previously that photophysical properties of this dye are dependent not only on the polarity or viscosity of the media but also on the specific solute−solvent interaction. Moreover, it serves as both a TICT-forming as well as hydrogen bond-forming dye in polar protic solvents. Although this molecule has a very strong propensity to form a TICT state, it does not show any kind of new band due to TICT. In the presence of TiO_2 nanoparticles, electron injection occurs from the TICT state of the dye to the conduction band of the nanoparticle, causing the appearance of a new band due to excited-state electron injection.[43] Very few studies are reported in the literature on the photophysics of 7-DCCA in different media.[44−48] To know how a hydrophilic dye such as 7-DCCA binds in the presence of macrocycles CB7 and HP-γ-CD, we have studied the photodynamics of this dye. We have used different spectroscopic techniques and isothermal titration calorimetry (ITC) to get a deeper understanding of the nature of inclusion processes involved between 7-DCCA and macrocyles. This study will be helpful to the understanding of how CB7 forms host−guest complexes with an anionic molecule and its differences when compared with cyclodextrin. A deeper understanding between the difference in interaction of anionic molecule with CB7 and cyclodextrins will be achieved through this work. Isothermal titration calorimetry experiments will help us to understand the difference in the nature of the binding of 7-DCCA with two highly water-soluble macrocycles in terms of enthalpy and entropy changes. The modulation of spectral properties of 7-DCCA in the presence of CB7 is opposite that of HP-γ-CD.

2. MATERIALS AND METHODS

7-DCCA was purchased from Sigma-Aldrich and used as received. 2-Hydroxypropyl-γ-cyclodextrin (HP-γ-CD) and cucurbit[7]uril were purchased from Sigma-Aldrich and used as received. For all the solution preparation, Millipore water was used. For studying the host−guest complexation, the dye concentration was maintained at ~3 × 10^{-6} M.

Ground-state absorption measurements were done by using ultraviolet−visible (UV−vis) spectrophotometer (model UV-2550, Shimadzu). The steady-state fluorescence emission measurements were carried out using Fluoromax-4P spectrofluorometer (Horiba Jobin Yvon). For absorption and fluorescence measurements, the path length of the used quartz cuvette was 1 cm. The fluorescence quantum yields of dye molecules were measured using the fluorescence quantum yield of coumarin 480 in water solution (ϕ_f = 0.66) as reference[49] by using the following equation:

$$\phi_f = \varphi_r \frac{I_s A_r n_s^2}{I_r A_s n_r^2} \quad (1)$$

where s and r stand for the sample and reference, respectively. Here, I stands for the integrated area under the fluorescence curve, A the absorbance of the sample at excitation wavelength, and n the refractive index of the medium. The time-resolved fluorescence emission decays were taken by using a picosecond time-correlated single-photon counting (TCSPC) technique. We have used a time-resolved fluorescence spectrophotometer from Edinburgh Instruments (model, LifeSpec-II, U.K.). We have used a picosecond diode laser with excitation wavelength at 405 nm. The instrument response function (IRF) of our system is ~80 ps. The fluorescence transients were detected at magic angle (54.7°) polarization using Hamamatsu MCP PMT (3809U) as a detector. The decays were analyzed using F-900 decay analysis software. The fluorescence anisotropy decay ($r(t)$) was measured by using the same instrument. The following equation was used to obtain r(t).

$$r(t) = \frac{I_{\parallel}(t) - GI_{\perp}(t)}{I_{\parallel}(t) + 2GI_{\perp}(t)} \quad (2)$$

where the emission intensities at parallel ($I_{\parallel}$) and perpendicular ($I_{\perp}$) polarizations were collected alternatively by fixing the time for both the decays. We have used motorized polarizers to collect the parallel and perpendicular decays. F-900 software was used to analyze the anisotropy decay. For time-resolved measurements, temperature was kept constant at 298 K by using a Peltier-controlled cuvette holders from Quantum Northwest (model, TLC-50). ^{1}H NMR spectral data were collected by a Bruker 500 MHz NMR spectrometer. Fourier transform infrared (FTIR) spectral data were collected in attenuated total reflection mode by using a PerkinElmer Spectrum 400 instrument. For isothermal titration calorimetry measurement, we have used an iTC_{200} microcalorimeter from GE healthcare. The temperature was kept constant at 298 K during the measurements.

3. RESULTS AND DISCUSSION

3.1. Steady-State Absorption and Fluorescence Emission Measurement. 7-DCCA is an acidic Coumarin dye and remains in deprotonated form in pure water,[46] with a prominent absorption band appearing at 409 nm. The pK_a value of the dye is 4.[46] Successive addition of HP-γ-CD causes a gradual blue shift of the absorption peak (Table 1). When the

dx.doi.org/10.1021/jp502944h | J. Phys. Chem. B 2014, 118, 9768−9781

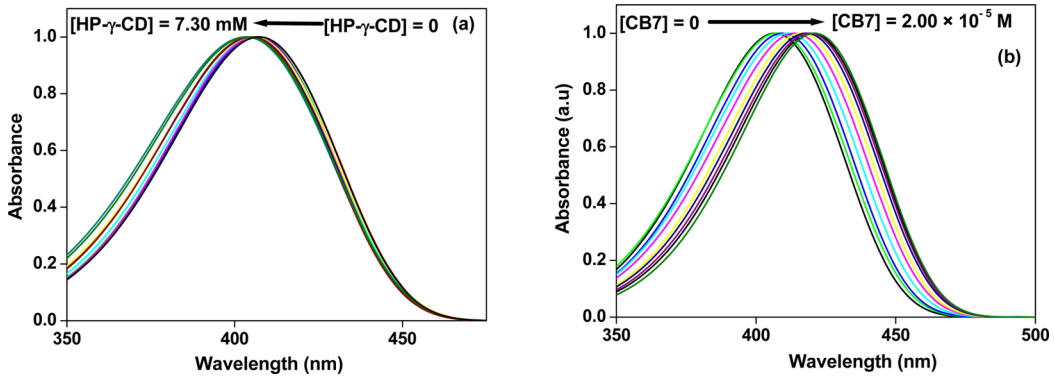

Figure 1. Change in absorption spectra of 7-DCCA with varying concentration of (a) HP-γ-CD and (b) CB7.

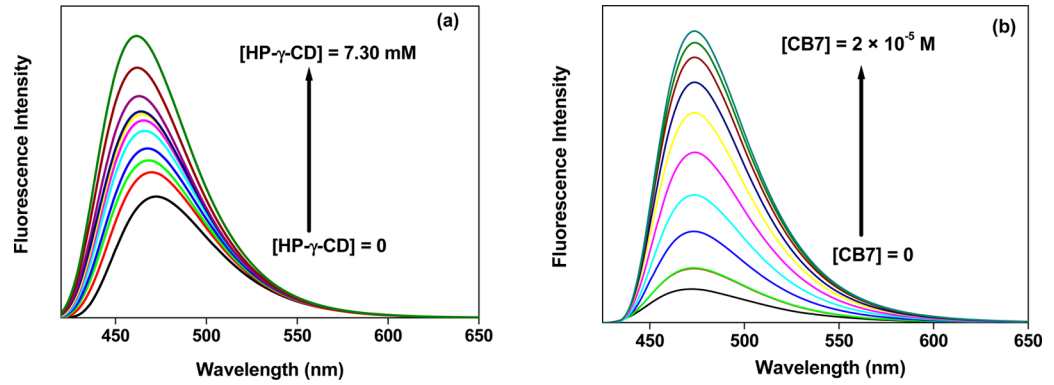

Figure 2. Emission spectral changes of 7-DCCA with varying concentration of (a) HP-γ-CD and (b) CB7.

concentration of HP-γ-CD reaches 6.93 mM, the absorption peak appears at 403 nm (Figure 1a, Table 1, and Figure S1a in the Supporting Information). The opposite effect is observed when the aqueous solution of 7-DCCA is treated with CB7. Gradual addition of CB7 causes the red shifting of the absorption spectra, and when the concentration of CB7 reaches 2.00×10^{-5} M, the absorption peak is red-shifted to 421 nm (Figure 1b, Table 1, and Figure S1b in the Supporting Information). Thus, addition of 2.00×10^{-5} M CB7 causes red shift of the absorption band by 12 nm. This red shifting of the absorption spectra indicates interaction is taking place between the dye and CB7.

We have studied the fluorescence emission properties of 7-DCCA in the presence of HP-γ-CD and CB7. We found that gradual addition of HP-γ-CD in the aqueous solution of 7-DCCA caused increase in the fluorescence quantum yield together with concomitant blue shift in the emission spectra from 472 nm in water to 461 nm in the presence of 6.93 mM HP-γ-CD (Figure 2a, Table 1). The fluorescence quantum yield (ϕ_f) gradually increases from 0.03 in water to 0.061 in the presence of 6.93 mM HP-γ-CD. This implies that 7-DCCA is facing a more restricted environment in the presence of HP-γ-CD (Table 1). As we have mentioned previously, TICT state formation is the main nonradiative decay process of 7-DCCA; therefore, in the presence of HP-γ-CD, the dye is expected to interact with the macrocyle. Hence, TICT state formation is strongly inhibited. Therefore, the fluorescent intensity as well as fluorescence quantum yields gradually increase. With gradual addition of HP-γ-CD, the dye probably gets incorporated inside the cavity of HP-γ-CD as the diameter of the dye is smaller than the cavity diameter of HP-γ-CD. Therefore, inhibition of TICT state formation causes an increase in the fluorescence quantum yield as well as fluorescence intensity. We had found that with gradual addition of the CB7 little change in the fluorescence emission peak was observed. In water, the dye shows an emission peak at 472 nm, and when CB7 concentration reaches 2.00×10^{-5} M, the fluorescence emission peak appears at 474 nm (Table 1, Figure 2b). With the gradual addition of CB7, the fluorescence quantum yield increases from 0.03 in pure water to 0.206 when the concentration of CB7 reaches 2.00×10^{-5} M (Table 1). Thus, fluorescence quantum yield increases by ∼7 times. This clearly implies that in the presence of CB7 the TICT state formation is strongly inhibited compared to that of HP-γ-CD. The cavity diameter of CB7 is 0.73 nm.[50] By using the method described by Edward, we have found that the diameter of 7-DCCA is 0.766 nm.[51] So the increase of the fluorescence quantum yield as well as the fluorescence intensity may be due to the formation of a host−guest complex between 7-DCCA and CB7. We have observed that with gradual addition of HP-γ-CD the full width at half maximum (fwhm) gradually decreases. When the concentration of HP-γ-CD reaches 6.93 mM, the fwhm of the emission spectra decreases to 2615 cm^{-1} from 2645 cm^{-1} in water (Figure S2a in the Supporting Information). Similarly, with gradual addition of CB7, the fwhm of the emission peak also decreases from 2645 cm^{-1} in water to 2375 cm^{-1} in the presence of 2.00×10^{-5} M CB7 (Figure S2b in the Supporting Information). This decrease in fwhm is due to a less polar environment faced by the dye molecule inside the cavity of macrocycles. In the case of CB7, we found that the increase in fluorescence intensity and fluorescence quantum yield is accompanied by very small or negligible shift in the emission spectra. This implies that complexation of 7-DCCA with CB7 may take place. This causes the prevention of conversion of emissive ICT state to

dx.doi.org/10.1021/jp502944h | J. Phys. Chem. B 2014, 118, 9768−9781

nonemissive TICT state. Therefore, the fluorescence emission quantum yield increases considerably together with the very small or negligible shift in the emission peak. This proposition is also supported by the work of Bhasikuttan et al.[20] The very small or negligible shift in the emission spectra is mainly due to the interaction between the dye and CB7 through the charge−dipole type interaction between partially positively charged $-NEt_2$ and the negatively polarized carbonyl portal of CB7. This is also supported by the work of Barooah et al.[13]

Therefore, on the basis of the results described in the above paragraph, one interesting feature of host−guest complexation was observed. We have observed almost no shift (slight red shift) in the fluorescence emission spectra when 7-DCCA formed a complex with CB7. However, in the presence of HP-γ-CD, the fluorescence emission spectra was blue-shifted. This is mainly due to deep immersion of the dye in the cavity of CB7. This is also supported by Nau and Mohanty.[52] The cavity of CB7 is highly hydrophobic and has low polarizability and polarity. The interaction of 7-DCCA with the hydrophobic cavity of CB7 changes the arrangement of the H-bond between water and carbonyl oxygen of the carboxylic acid group of 7-DCCA. This may be responsible for the large red shift of the absorption spectra but the small red shift in the fluorescence emission spectra. Our proposition also gets support from the work of Gupta et al.[30] The blue shift in both the absorption and emission spectra of 7-DCCA in the presence of HP-γ-CD is not entirely due to the presence of a less polar environment inside the hydrophobic cavity. If a less polar environment were the only driving factor for the spectral properties of 7-DCCA, then a large blue-shifted emission would be observed in the presence of CB7. Here, beside the less polar environment of the hydrophobic cavity of HP-γ-CD, H-bonding interactions between 7-DCCA and HP-γ-CD also have caused the blue shifting of the absorption and emission spectra. However, because of trapping of the diethylamino group inside the hydrophobic cavity of CB7 and HP-γ-CD, the formation of a TICT state is restricted. Hence, this increases the fluorescence quantum yield of 7-DCCA. Similar blue shift in the guest spectrum on forming direct H-bonding interaction with cyclodextrin and subsequent increase in fluorescence quantum yield and excited-state lifetime were previously reported in the literature.[53,54]

The surprising feature to be observed here is that after the addition of 6.93 mM HP-γ-CD, the fluorescence quantum yield increases from 0.03 in water to 0.061, whereas the fluorescence quantum yield increases to 0.206 after the addition of 2.00×10^{-5} M CB7. This shows the environment faced by 7-DCCA inside the cavity of CB7 is more restricted than that in HP-γ-CD. The greater enhancement of fluorescence emission in the presence of CB7 is probably due to the confinement of 7-DCCA inside a highly rigid environment of cavity of CB7. Moreover, the dye experiences very low polarizability inside the cavity of CB7. The polarizability as well as the refractive index inside the cavity is very close to that of the gas phase.[52] The high rise in the fluorescence quantum yield of 7-DCCA in CB7 compared to that in HP-γ-CD is mainly due to the presence of both charge−dipole and hydrophobic interactions. This is supported by the work of Li et al.[24] Increase in fluorescence quantum yield arises mainly because of the inhibition of the nonradiative decay processes of the excited state of 7-DCCA by restricting the molecule in the hydrophobic cavity of macrocycles. This causes the inhibition of the TICT state formation in the excited state. The inhibition of the excited state also depends on the degree of penetration of the dye inside the cavity of macrocycles. In the case of complex formation between 7-DCCA and HP-γ-CD, H-bonding interaction plays a prominent role. This H-bonding interaction between the dye and HP-γ-CD causes a shallow degree of penetration of the dye inside the cavity of HP-γ-CD. On the other hand, deep penetration of the dye inside the highly hydrophobic cavity strongly prevents the TICT state formation. This causes the greater increase of fluorescence quantum yield of 7-DCCA in CB7 compared to that in HP-γ-CD.

3.2. Determination of the Binding Constants and Stoichiometry. The binding interaction between the dye and macrocycles occurs in successive steps. The equilibrium of complex formation can be given by the following equations:

$$\text{dye} + \text{macrocycle} \leftrightarrow \text{dye}\cdot\text{macrocycle}$$

$$\text{dye}\cdot\text{macrocycle} + \text{macrocycle} \leftrightarrow \text{dye}\cdot(\text{macrocycle})_2$$

The method for determining the binding constant values is a nonlinear least-squares regression analysis, in which the data are directly fitted by using the relevant equation.[55] In this approach, the initial values of the unknown parameters are taken from linear fitted results using the Benesi−Hildebrand equation. For the 1:1 and 1:2 guest:host complex, the binding equation can be represented as

$$F = \frac{F_0 + F_1K_1[H]_0}{1 + K_1[H]_0} \tag{3}$$

$$F = \frac{F_0 + F_1K_1[H]_0 + F_2K_1K_2[H]_0^2}{1 + K_1[H]_0 + K_1K_2[H]_0^2} \tag{4}$$

where F, F_0, F_1, F_2, K_1, K_2, and $[H]_0$ stand for observed fluorescence intensity, fluorescence intensity in absence of host, fluorescence intensity when 1:1 binding has completed, fluorescence intensity when 1:2 binding has completed, binding constant for 1:1 binding, binding constant for 1:2 binding, and concentration of the added host, respectively. Using the above equations, we have found that 7-DCCA forms 1:2 complex (guest:host) with HP-γ-CD. The binding constants for 1:1, 1:2 complexes are found to be 1580 ($\pm$620) M^{-1} (K_1), 9 ($\pm$6) M^{-1} (K_2) respectively, indicating very weak interaction in the case of 1:2 complex formation (Table 2, Figure 3a). We have found that 7-DCCA forms 1:2 complex with CB7. By using eq 4, we have found a reasonably well-fitted curve with an R^2 value of 0.999 (Figure 3b). The binding constants for 1:1 and 1:2 (guest:host) complexes are 1.12 ($\pm$0.5) $\times 10^5$ M^{-1} and 2.34 ($\pm$0.9) $\times 10^5$ M^{-1}, respectively (Table 2, Figure 3b). This indicates stronger interaction between 7-DCCA and CB7 compared to that with HP-γ-CD.

Table 2. Binding Constant Values for the Interaction between 7-DCCA and HP-γ-CD and CB7

sr no.	system	$K_{1:1}$ (M^{-1})	$K_{1:2}$ (M^{-1})
1	7-DCCA in HP-γ-CD	1580 ($\pm$620)	9 ($\pm$6)
2	7-DCCA in CB7	1.12 ($\pm$0.5) $\times 10^5$	2.34 ($\pm$0.9) $\times 10^5$

3.3. Time-Resolved Emission Measurement. We have studied the time-resolved emission properties of 7-DCCA in the presence of macrocycles HP-γ-CD and CB7 (Figure 4a,b). In neat water, 7-DCCA shows two distinct components. One is a fast component of 0.130 ns, and the other one is a slow

dx.doi.org/10.1021/jp502944h | J. Phys. Chem. B 2014, 118, 9768−9781

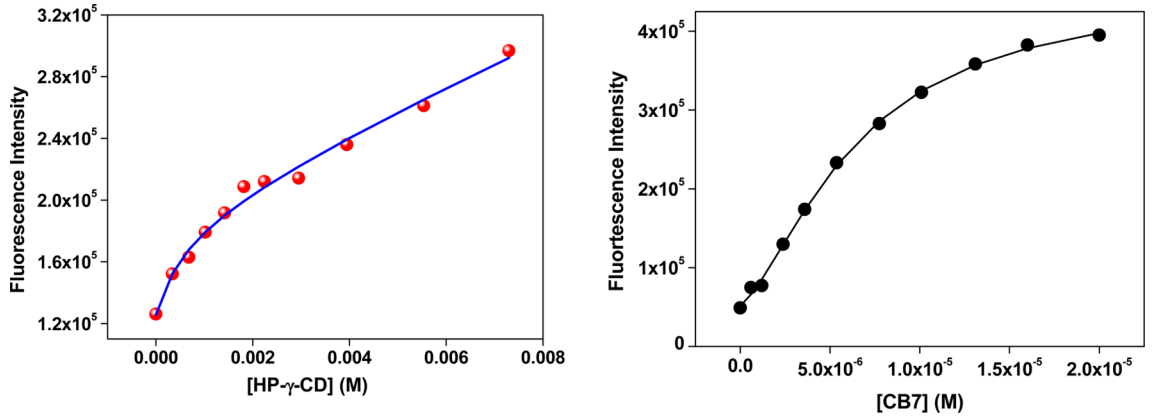

Figure 3. Binding interaction between 7-DCCA with HP-γ-CD and CB7 forming 1:2 complexes.

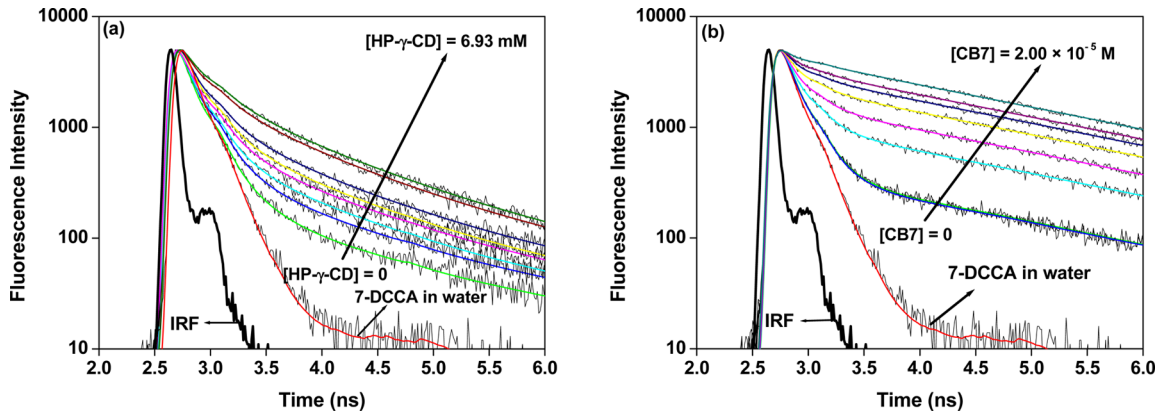

Figure 4. Fluorescence emission decays of 7-DCCA with varying concentration of (a) HP-γ-CD and (b) CB7.

Table 3. Fluorescence Lifetime Values of 7-DCCA ($\sim 3 \times 10^{-6}$ M) in the Presence of HP-γ-CD and CB7

sr no.	system	τ_1 (ns)	a_1	τ_2 (ns)	a_2	τ_3 (ns)	a_3	$\langle\tau_f\rangle^a$ (ns)	χ^2
1	7-DCCA in water	0.130	0.995	–	–	2.759	0.005	0.140	1.071
2	7-DCCA in water + 1.35 mM HP-γ-CD	0.138	0.894	0.744	0.086	2.505	0.020	0.237	1.023
3	7-DCCA in water + 3.75 mM HP-γ-CD	0.148	0.781	0.738	0.182	2.377	0.037	0.338	1.006
4	7-DCCA in water + 6.93 mM HP-γ-CD	0.170	0.698	0.803	0.250	2.414	0.052	0.443	1.040
5	7-DCCA in water + 1.20×10^{-6} M CB7	0.132	0.961	–	–	2.181	0.039	0.210	1.037
6	7-DCCA in water + 5.37×10^{-6} M CB7	0.135	0.689	–	–	2.153	0.311	0.762	1.041
7	7-DCCA in water + 1.01×10^{-5} M CB7	0.137	0.548	–	–	2.158	0.452	1.050	1.086
8	7-DCCA in water + 2.00×10^{-5} M CB7	0.138	0.390	–	–	2.155	0.610	1.368	1.038

$^a\langle\tau_f\rangle = a_1\tau_1 + a_2\tau_2 + a_3\tau_3$

component of 2.759 ns (Table 3). The weight percentage of the slow component is only 0.5%, and that of the fast component is 99.5%. The origin of these components has been described previously.[43,46] After the addition of HP-γ-CD, we observed that another component is generated. This component falls in an intermediate range of fast and slow components. With gradual increase in the concentration of HP-γ-CD, we have found that the weight percentage of the fast component gradually decreases (Figure S3a in the Supporting Information), whereas the time constant values gradually increase (Table 3). The slight increase in the time scale of this fast component is mainly due to the interaction with the HP-γ-CD. On the other hand, the time constant (τ_2) and weight percentage (a_2) of the intermediate component increases with addition of HP-γ-CD (Figure S3a in the Supporting Information). The appearance of this new component is mainly due to the formation of a complex with HP-γ-CD. The time constant of the slowest component in water gradually decreases in a regular pattern from 2.759 ns in pure water to 2.414 ns in the presence of 6.93 mM HP-γ-CD. At the same time the weight percentage of the slowest component gradually increases from 0.5% in water to 5.2% in the presence of 6.93 mM HP-γ-CD (Figure S3a in the Supporting Information). This decrease in the decay time constant of the slowest component together with the increase in the weight percentage of this component is due to the formation of a complex between the dye and the HP-γ-CD. The presence of these three components in the presence of HP-γ-CD is indicative of the existence of three different population types of 7-DCCA. Here, we have attributed these three components as follows:

(a) The fast component is due to the free dye.

dx.doi.org/10.1021/jp502944h | J. Phys. Chem. B 2014, 118, 9768−9781

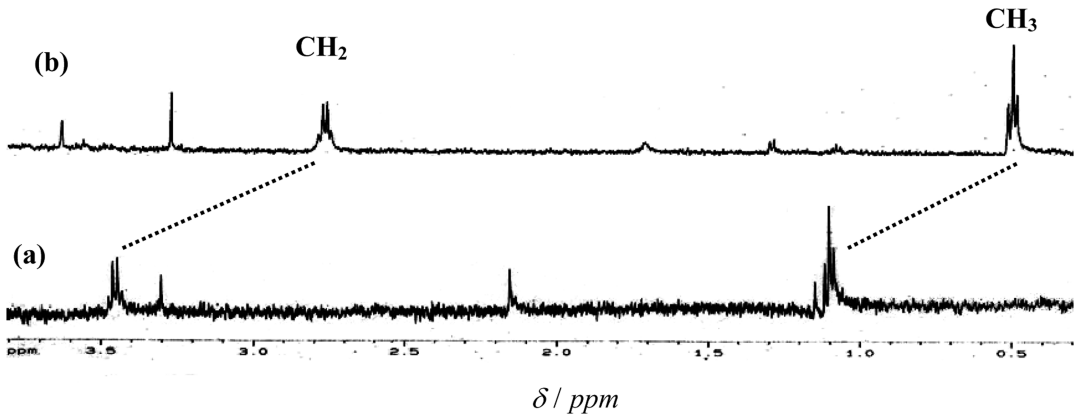

Figure 5. ^{1}H NMR spectra (500 MHz) of ~100 μM 7-DCCA in D_2O in (a) free dye and in the presence of (b) 1 mM CB7.

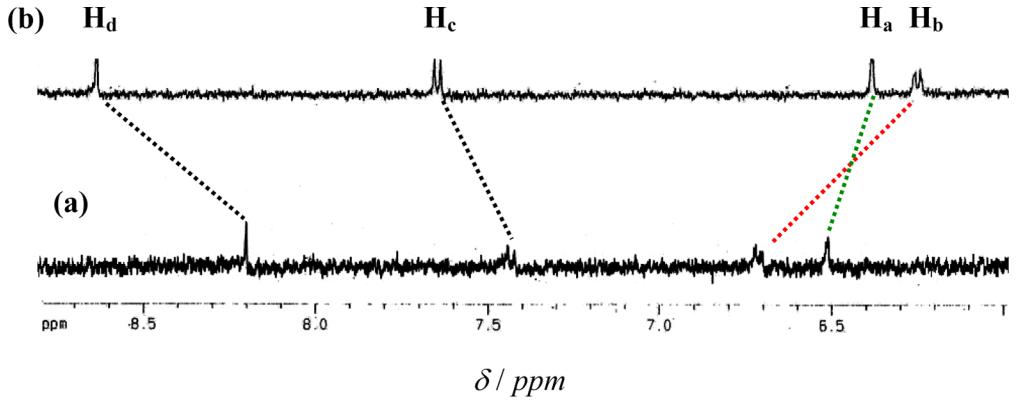

Figure 6. ^{1}H NMR spectra (500 MHz) of ~100 μM 7-DCCA in D_2O in (a) free dye and in the presence of (b) 1 mM CB7. H_a, H_b, H_c, and H_d are shown in Scheme 1.

(b) The intermediate component is due to the 1:1 complex formation.
(c) The slow component is due to the 1:2 complex formation.

This proposition also gets support from the work of Martin et al.[56] On the other hand, the addition of CB7 in the aqueous solution of 7-DCCA does not result in the appearance of any new component. The fast component remains almost constant in time scale, although the weight percentage of that component gradually decreases (Table 3). This indicates that the weight percentage of the emissive ICT state gradually decreases with the gradual increase in the concentration of CB7 (Figure S3b in the Supporting Information). The slowest component shows a decrease in its time constant value with increase in the concentration of CB7, whereas the weight percentage of the slow component gradually increases, from 0.5% in water to 61% in the presence of 2.00×10^{-5} M CB7 (Figure S3b in the Supporting Information). Thus, the weight percentage of the slow component gradually increases by ~122 times, whereas the time constant decreases by 0.604 ns because of addition of 2.00×10^{-5} M CB7 in the aqueous solution of 7-DCCA. This indicates that addition of CB7 in a gradual manner causes the formation of the complex between the dye and supramolecular host CB7. For both the macrocycles, however, the average fluorescence decay time gradually increases with gradual addition of macrocycles. The average fluorescence decay time of 7-DCCA gradually increases from 0.140 ns in water to 0.443 ns in the presence of 6.93 mM HP-γ-CD. On the other hand, in the presence of 2.00×10^{-5} M CB7, the average fluorescence decay time increases to 1.368 ns. This indicates that in the presence of CB7 the dye 7-DCCA experiences a more restricted environment than in the presence of HP-γ-CD. This restricted environment causes inhibition of TICT state formation. This inhibition of TICT state formation is responsible for the increase in the fluorescence decay times. We have mentioned previously that the TICT state formation is the main nonradiative deactivation pathway. The radiative and nonradiative rate constants are given by the following equations:

$$k_r = \frac{\phi_f}{\langle \tau_f \rangle} \tag{5}$$

$$\frac{1}{\langle \tau_f \rangle} = k_r + k_{nr} \tag{6}$$

where ϕ_f is the fluorescence quantum yield and k_r and k_{nr} are the radiative and nonradiative decay rate constants, respectively. For the macrocycle HP-γ-CD, the nonradiative decay rate constant k_{nr} decreases in a regular way and varies from 6.93×10^9 s^{-1} in water to 2.12×10^9 s^{-1} in the presence of 6.93 mM HP-γ-CD (Table 1, Figure S4 in the Supporting Information). On the other hand, addition of 2.00×10^{-5} M CB7 causes decrease of the k_{nr} value from 6.93×10^9 s^{-1} in water to 5.80×10^8 s^{-1} in the presence of 2.00×10^{-5} M CB7. This indicates that the macrocycle CB7 provides an environment that is more hydrophobic and restricted than that of the HP-γ-CD. Our proposition is supported by the higher binding constant with

dx.doi.org/10.1021/jp502944h | J. Phys. Chem. B 2014, 118, 9768−9781

Scheme 1. Schematic Representation of 7-DCCA, Cucurbit[7]uril, and 2-Hydroxypropyl-γ-cyclodextrin

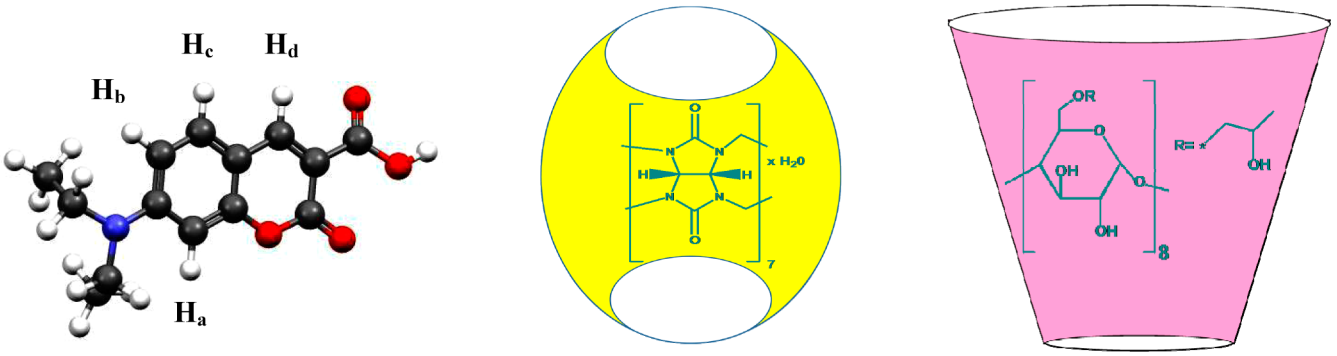

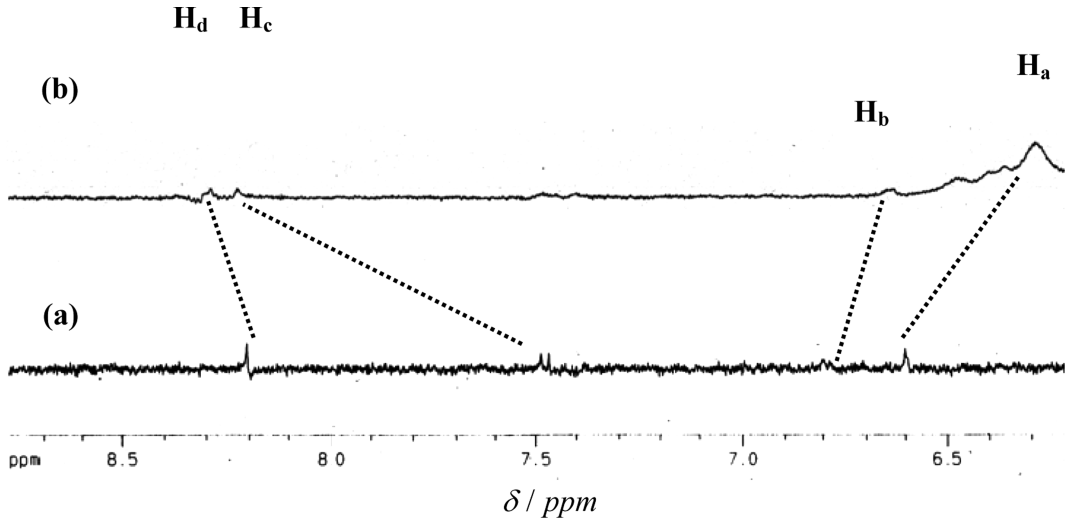

Figure 7. ^{1}H NMR spectra (500 MHz) of ∼50 μM 7-DCCA in D_2O in (a) free dye and in the presence of (b) 125 mM HP-γ-CD.

CB7 than with HP-γ-CD. The residuals of fitted decays are shown in Figures S5 and S6 in the Supporting Information.

However, in both cases, the components of fluorescence decay times gradually change because of gradual addition of macrocycles. Addition of macrocycles causes the formation of complexes with the dye, thereby causing the restriction of twisting of diethylamino group of the dye to produce the TICT state. This inhibition of formation of the TICT state causes the nonradiative decay to be suppressed by a competitive fluorescence radiative decay process causing the increase in fluorescence decay time.

3.4. ^{1}H NMR Studies of the Host−Guest Complexation. To further investigate the host−guest complexation between 7-DCCA and the two macrocycles, we have used the ^{1}H NMR spectroscopic technique. Comparatively greater solubility of 7-DCCA in D_2O than other hydrophobic coumarins makes it possible to study ^{1}H NMR in D_2O. In D_2O, in the presence of CB7, the methyl (δ 1.13) and methylene (δ 3.42) protons of the $-NEt_2$ group are found to show 0.63 and 0.65 upfield shift, respectively (Figure 5). This clearly demonstrates the complete inclusion of the $-NEt_2$ group of the dye deep inside the cavity of CB7. The aromatic protons H_a (δ 6.59) and H_b (δ 6.79) show 0.2 and 0.53 upfield shifts, respectively, and H_c (δ 7.48) shows a 0.16 downfield shift upon addition of CB7 (Figure 6). This clearly indicates that although H_b is deeply buried inside the hydrophobic cavity of CB7, H_a resides comparatively near the portal of CB7. However, the downfield shift of H_c shows the effect of deshielding of carbonyl portals. Again, the H_d (δ 8.20) shows 0.44 downfield shift in the presence of CB7. This clearly shows that the proton H_d resides near the carbonyl portal of CB7, which exerts its effect of deshielding but outside the cavity of CB7.

When HP-γ-CD is added to the 7-DCCA in D_2O, it is found that H_a (δ 6.59) and H_b (δ 6.79) undergo 0.32 and 0.19 upfield shift, respectively (Figure 7), indicating that these protons are buried inside the hydrophobic cavity of HP-γ-CD. The H_c and H_d protons show a downfield shift on addition of HP-γ-CD. This indicates the ground-state interaction between the dye 7-DCCA and HP-γ-CD.

3.5. Interaction between 7-DCCA with Macrocycles: Ground-State versus Excited-State Binding? When discussing the host−guest complexation in the excited state, mainly three rates are important. These are as follows: (a) the rate of inclusion of the guest inside the cavity of host macrocycle, (b) the rate of exclusion of the guest from the cavity of host macrocycle, and (c) the rate of decay of the excited-state host.

When the excited-state lifetime is short, the rate of excited-state decay may be significantly faster than either the rate of inclusion or rate of exclusion. Under such circumstances, only those guest molecules that are encapsulated inside the cavity of the macrocycle are excited by absorbing light. Under such conditions, the rate of inclusion, rate of exclusion, as well as the binding interaction will depend upon the ground-state binding. However, electronic excitation of the guest by the absorption of

dx.doi.org/10.1021/jp502944h | J. Phys. Chem. B 2014, 118, 9768−9781

light may also destabilize the complex and may also eventually lead to the dissociation of the complex. This phenomenon is prominent when the excited-state binding constant values are lower than that of the ground state, i.e., the excited-state binding interaction is weaker than that of ground state. Again, when the excited-state lifetime is high, it may be possible that the guest is excited outside the cavity and enters into the macrocycle cavity during excited-state lifetime. Under such conditions, the rates of inclusion and exclusion from the cavity may be significantly different in the excited state compared to those in the ground state. This causes the different values of binding constants in the ground and excited states.[53]

The binding constant values obtained from the fluorescence studies indicate the extent of binding interaction between the dye and macrocycle. The binding constant values are the most important measurable property for understanding the total driving force of inclusion. To obtain a highly stable host−guest complex, the rate of inclusion (k_{in}) of the guest into the host must be significantly larger than the rate of exclusion of the dye from the host cavity (k_{out}). The binding constant value is represented as $K = k_{in}/k_{out}$.[57] This equation can be further represented as $K = \tau_{out}/\tau_{in}$. τ_{in} and τ_{out} stand for the time scale for inclusion and exclusion of the guest molecule in the host macrocycles. Ground-state complex formation between 7-DCCA and macrocycles has been proven by ^{1}H NMR, ITC, and FTIR spectroscopic methods. In the case of the 7-DCCA−CB7 complex, the overall binding constant value in the ground state (K_1K_2) is $\sim 7 \times 10^{10}$ (Table S1 in the Supporting Information). Absence of isosbestic point in absorption spectra makes it difficult for us to determine the kinetics of association and dissociation by the method proposed by Zhang et al.[58] We can determine a rough estimate of how long the dye molecule resides inside the cavity of macrocycles. In our study, we have used the ^{1}H NMR spectra to observe the shifts of δ values to understand complexation behavior. The time scale of ^{1}H NMR spectra to observe the shifts of δ value is in the microsecond to millisecond range. Very strong binding between 7-DCCA and CB7 clearly indicates that the exchange of dye between the complex and free dye in solution is extremely sluggish and the dye mainly remains in the cavity of the CB7 for a time scale comparable to or slower than the ^{1}H NMR technique. Therefore, the time τ_{in} is extremely fast compared to the fluorescence excited-state decay time of 7-DCCA. Here, we have found that there are significant differences between the K_1 and K_2 values between the ground- and excited-state binding of 7-DCCA with CB7. This may be due to fact that 7-DCCA excited outside the cavity enters inside the hydrophobic cavity of CB7 during the excited-state lifetime. This causes the difference between the rates of inclusion and exclusion of 7-DCCA in the excited state and those in the ground state. This may account for the difference between the ground-state binding constants (K_1 and K_2) and those of excited state.

In the case of complex formation of 7-DCCA with HP-γ-CD, the overall ground-state binding constant is $\sim 4 \times 10^2$ (Table S1 in the Supporting Information). Thus, the τ_{in} and τ_{out} values in the ground state are higher than the fluorescence lifetime of the guest. This accounts for the fact that the 7-DCCA complexed with HP-γ-CD absorbs light to get excited. Under such circumstances, the rate of inclusion, rate of exclusion, as well as binding with the HP-γ-CD macrocycle are dependent on ground-state binding.

3.6. FTIR Studies of the Host−Guest Complexation. We have used the FTIR technique to get further insight into the complex formation between the dyes 7-DCCA with macrocycles. We have found that an aqueous solution of 7-DCCA shows a broad peak at 3392 cm^{-1}. This peak is attributed to the O−H of −COOH group present in the coumarin, which is extensively hydrogen-bonded with the surrounding water molecules. This causes the broad spectra near 3400 cm^{-1}. There are also peaks in the range of 2800−3000 cm^{-1}. These peaks originate because of the presence of aromatic and aliphatic C−H bonds. The peak due to the carbonyl group appears at 1636 cm^{-1}. The peak due to C═C stretching appears at 1520 cm^{-1}. Another broad and weak peak appears at ∼1342 cm^{-1}. This is probably due to the presence of a N−C (aromatic) bond. The FTIR spectrum of HP-γ-CD is shown in Figure S7 in the Supporting Information. The spectrum shows a broad and strong band at 3423 cm^{-1}. After the addition of 2.80 mM HP-γ-CD in the solution of 7-DCCA, the band at 3392 cm^{-1} undergoes a shift to 3423 cm^{-1}. This indicates the interaction between 7-DCCA with HP-γ-CD. This causes the disruption of the extensive hydrogen bonding between 7-DCCA and the surrounding water molecules. Moreover, addition of 2.80 mM HP-γ-CD makes the peak at 3000 cm^{-1}, which is probably due to an aromatic C−H bond, sharp relative to the broad peak at almost the same wavenumber before the addition of HP-γ-CD. Moreover, the peak due to vinyl C−H bond (C═C−H) was not as prominent in the free dye, but becomes prominent at 3011 cm^{-1} after the addition of 2.80 mM HP-γ-CD. This highlights the interaction between the dye and HP-γ-CD. The peak at 2952 cm^{-1} in 7-DCCA is also shifted to 2941 cm^{-1} in the presence of 2.80 mM HP-γ-CD. These results indicate that the C−H (aliphatic) bonds tend to enter the hydrophobic cavity of HP-γ-CD during the inclusion of the $-NEt_2$ group inside the HP-γ-CD. During this inclusion, the van der Waals interaction was operating. This shifting because of the van der Waals interaction is supported by the work of Sambasevam et al.[59] It may also happen that aliphatic H atoms form initially the hydrogen bonding with the oxygen atom of OH group of the cyclodextrin during the complex formation. The peak due to the carbonyl group at 1636 cm^{-1} shifts to 1640 cm^{-1} after the addition 2.80 mM HP-γ-CD. This further indicates that the carbonyl group is exposed to the environment, where extensive hydrogen bonding interaction between carbonyl group with the surrounding medium breaks down. This enhances the wavenumber of the carbonyl bond. Again, the peak at 1520 cm^{-1} of 7-DCCA shifted to 1524 cm^{-1}, showing that the hydrophobic interaction is taking place between the dye and macrocycle. This happens because of the inclusion of the aromatic part of 7-DCCA inside the cavity of HP-γ-CD. After the addition of 6.93 mM HP-γ-CD, the peak at 3423 cm^{-1} remains the same. On the other hand, the peak at 3000 cm^{-1} undergoes a shift at 2992 cm^{-1}. Moreover, both the peaks at 2940 and 2830 cm^{-1} (after the addition of 2.80 mM HP-γ-CD) undergo a shift to 2944 and 2837 cm^{-1} after the addition of 6.93 mM HP-γ-CD. This type of shift is due to the hydrophobic interaction between the dye and HP-γ-CD.

We have studied the host−guest complexation between 7-DCCA and CB7 by using FTIR spectroscopy (Figure S8 in the Supporting Information). The broad and strong band at 3392 cm^{-1} is due to the presence of O−H of the carboxylic acid group and shows a shift toward the higher wavenumber at 3417 cm^{-1}. This result highlights the interaction between 7-DCCA and CB7 and disruption of the extensive H-bonding network between the dye and surrounding water medium. This shows

dx.doi.org/10.1021/jp502944h | J. Phys. Chem. B 2014, 118, 9768−9781

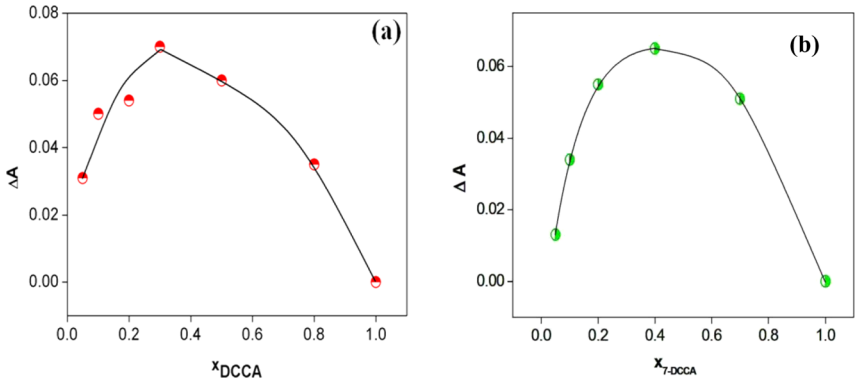

Figure 8. Job's plot by continuous variation method for 7-DCCA in the presence of (a) HP-γ-CD and (b) CB7.

that the carboxylic acid part of 7-DCCA entered the highly hydrophobic cavity of CB7. At the same time, the peak at 2992 cm^{-1} also shifted to 3015 cm^{-1}. This indicates that the aromatic C−H bonds enter the cavity of CB7 with low polarizability. This was previously confirmed by the ^1H NMR studies and is reinforced by FTIR study. Moreover, the weak band at 2992 cm^{-1} after the addition of CB7 becomes sharp together with the prominence of the vinyl C−H (C═C−H). This confirmed the interaction between 7-DCCA and CB7 and inclusion of $-NEt_2$ group inside the cavity of CB7. Moreover, the shifting of the carbonyl peak from 1636 to 1632 cm^{-1} is also indicative of the interaction between the dye and CB7.

3.6.1. Comparison. The most interesting feature of the inclusion phenomenon is the extent to which the dye molecule penetrates inside the cavity of the macrocycles and how the host cavities affect the binding interaction. From the shift of the stretching frequency of C═C bond of the dye on complexation, it is clear that the extent of inclusion of the aromatic part of 7-DCCA is greater in CB7. In HP-γ-CD, the peak at 1520 cm^{-1} is shifted to 1524 cm^{-1}, whereas in the case of CB7, this peak shifts up to 1533 cm^{-1}. This happens because of the greater interaction between the more hydrophobic cavity of CB7 and the dye. This implies that greater penetration into the more hydrophobic CB7 cavity increases the force constant of the C═C bond to a greater extent than in HP-γ-CD. This is also evident from the higher binding constant value in the presence of CB7 compared to that of HP-γ-CD. However, shifting of the −OH stretching frequency toward longer wavenumber is observed in both the macrocycles. There are also significant differences between the shifting of the carbonyl group stretching frequencies. In the case of HP-γ-CD, the carbonyl stretching frequency initially increases because of addition of 2.80 mM HP-γ-CD, from 1636 to 1640 cm^{-1}. It may be possible that the rupture of the extensive H-bond network between the dye and water molecules and establishment of weak H-bonding network between the dye and HP-γ-CD take place. For this reason, both O−H and carbonyl stretching frequencies shifted to the higher wavenumber because change of H-bonding strength also increases the force constant of the bonds. The shifting of bond-stretching frequency toward the longer wavenumber region due to weak H-bonding interaction has been reported in the literature.[60] On the other hand, in the case of CB7, a similar kind of shift of O−H stretching frequency was observed because of complex formation. Therefore, this result demonstrates the inclusion of the carboxylic acid group of 7-DCCA inside the cavity of CB7. Unlike the 7-DCCA−HP-γ-CD complex, in the 7-DCCA−CB7 complex, the peak due to the aliphatic C−H stretching does not shift after complex formation. This indicates that H-bond formation was not taking place between the aliphatic C−H bonds and CB7. The weak broad band at 3000 cm^{-1} which constitutes the aromatic C−H group shows a shift to 3015 cm^{-1} together with a significant enhancement of intensity. This indicates greater degree of penetration of the aromatic ring of 7-DCCA inside the hydrophobic cavity of CB7 compared to that in HP-γ-CD. This is also substantiated by the high binding constant value of 7-DCCA with CB7. A weak band due to C−N bond stretch (∼1342 cm^{-1}) moves to a higher wavenumber value (∼1366 cm^{-1}) with concomitant intensification of the band on complexation with 6.93 mM HP-γ-CD. The band also gets sharper because of complex formation. This signifies the inclusion of the $-NEt_2$ group inside the hydrophobic cavity of HP-γ-CD. A similar observation is also made in the case of the 7-DCCA−CB7 complex, with the exception that the band has moved to a higher wavenumber (1370 cm^{-1}). Moreover, the C−N bond has now become more intense and sharper than that in the 7-DCCA−HP-γ-CD complex. This indicates deeper penetration of the $-NEt_2$ group inside the highly hydrophobic cavity of CB7 compared to that in HP-γ-CD. This is quite expected as we have seen greater increase of fluorescence lifetime and fluorescence quantum yield in the case of 7-DCCA·$(CB7)_2$ complex compared to that of 7-DCCA·$(HP\text{-}\gamma\text{-}CD)_2$.

3.7. Determination of Stoichiometry of the Complex by Job's Plots. The stoichiometry of host−guest complexes of 7-DCCA with HP-γ-CD and CB7 has been examined by using the Job's method of continuous variation.[61] Here the plots of ΔA (difference of absorbance) against $x_{7\text{-DCCA}}$ (the mole fraction of the dye) show their maximum at 0.3 and 0.39 for 7-DCCA−HP-γ-CD ([7-DCCA] + [HP-γ-CD] = 1.91×10^{-4} M) and 7-DCCA−CB7 ([7-DCCA] + [CB7] = 1.91×10^{-4} M) complexes, respectively, showing 1:2 (guest:host) composition of the complexes for both cases. The Job's plots are shown in panels a and b of Figure 8 for HP-γ-CD and CB7 complexes, respectively.

3.8. Study of Binding Thermodynamics of 7-DCCA with Macrocycles Using Isothermal Titration Calorimetric Measurements. The isothermal titration calorimetry (ITC) technique was used to study the binding interaction between the dye and macrocycles. The calorimetric measurement also helped us to determine the thermodynamic parameters and also the nature of binding between 7-DCCA with two macrocycles HP-γ-CD and CB7. The interaction between the guest (dye) and host (macrocycle) proceeds to

dx.doi.org/10.1021/jp502944h | J. Phys. Chem. B 2014, 118, 9768−9781

reach equilibrium. The equilibrium can be represented as follows:

$$m\,\text{dye} + n\,\text{macrocycle} \leftrightarrow \text{dye}_m\cdot\text{macrocyle}_n$$

where m, n = 1, 2, 3, etc.

We have previously showed from fluorescence data that the dye forms 1:2 (guest:host) complexes with both HP-γ-CD and CB7. Let us consider first the interaction of 7-DCCA with HP-γ-CD. The interaction between the dye 7-DCCA and HP-γ-CD is of a 1:2 nature as obtained from ITC measurement. Here, data were fitted by two-site sequential binding model as shown in Figure 9a. From the data obtained, we have found that the

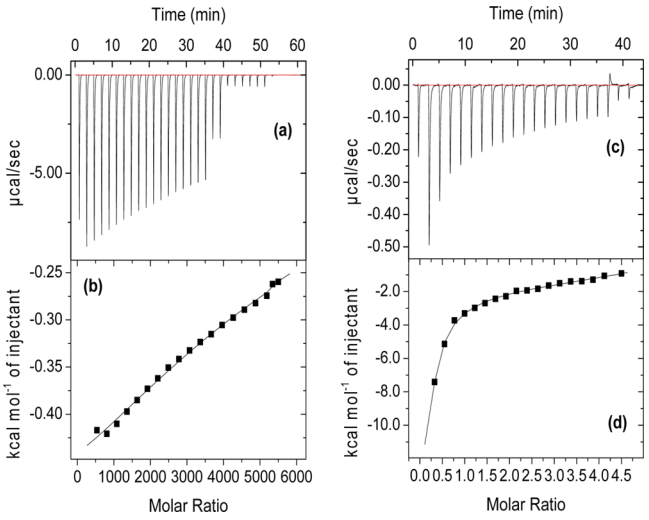

Figure 9. (a) ITC isotherm for the injection of 0.12 M HP-γ-CD solution in 5 μM 7-DCCA solution at 298 K. (b) Data points represent integrated heats of interaction as a function of molar ratio, and the solid line represents the line of best fit. (c) ITC isotherm for the injection of 450 μM CB7 solutions in 20 μM 7-DCCA solutions at 298 K. (d) Data points represent integrated heats of interaction as a function of molar ratio, and the solid line represents the line of best fit.

binding constant values are K_1 = 65 (±37) M^{-1} and K_2 = 6 (±1) M^{-1}. For both binding sequences, the enthalpy and entropy values are negative and are tabulated in Table S1 in the Supporting Information. For the first sequence, in which K_1 = 65 (±37)M^{-1}, the binding process is enthalpy driven as indicated by $|H| > |T\Delta S|$. The small value of the binding constant for this step is due to the fact that the contributions from both the enthalpy and entropy are almost equal and the Gibb's free energy of binding is −2.46 kcal mol^{-1} (−10.33 kJ mol^{-1}) to produce 7-DCCA−HP-γ-CD complex. For the step where K_2 = 6 (±1) M^{-1}, the binding process is enthalpy driven as $|H| > |T\Delta S|$. The Gibb's free energy of formation of 7-DCCA−(HP-γ-CD)$_2$ complex is −1.06 kcal mol^{-1} (−4.45 kJ mol^{-1}). Ross and Subramanian reported that the main reasons of negative enthalpy and entropy changes are the nonbonded (van der Waals) interaction, hydrogen bond formation in low dielectric media, and protonation together with association.[62] Here, highly exothermic complex formation is characterized by the reduction of entropy in both steps. This can be attributed to the large restriction of the translational and conformational freedom. This is supported by the work of Liao et al.[63] Another reason which may be responsible for the decrease of entropy is the water molecules inside the cavity of HP-γ-CD are highly disordered because of their inability to form a hydrogen-bonding network. This type of water molecule that does not have full complement of H-bonds are enthalpy-rich water molecules. After the complex formation, when these trapped water molecules are released from the cavity, a complete H-bonding network is promptly attained, together with the release of heat. This leads to the decrease in the disorder, thereby leading to the decrease in entropy.[64] So all these factors contribute to the formation of the 7-DCCA·(HP-γ-CD)$_2$ complex. Although the formation of an intermolecular hydrogen bond between the dye and cyclodextrin is quite improbable because of the strong hydration of hydrogen bonding sites, it is possible because of the close proximity of the dye and cyclodextrin during the complex formation.[65,66]

In the case of complex formation between 7-DCCA and the macrocycle CB7, the data points are fitted by the two sets of sites model (Figure 9b). This further confirms the formation of a 1:2 (guest:host) complex. The thermodynamic parameters are tabulated in Table S1 in the Supporting Information. Here the values of binding constants are sufficiently large because of high complex formation ability of CB7, as mentioned earlier. Here the first step of 1:1 complex formation is an enthalpically and entropically favorable process, although this step is enthalpy driven as evident from $|H| > |T\Delta S|$. In this step, we observe that entropy change is positive. This positive change of entropy may be attributed to the expulsion of the high-energy water molecules from the cavity of CB7. The cavity of CB7 does not allow the trapped cavity water molecules to orient them in an energetically favorable H-bonding network. Biedermann et al. calculated the potential energy of release of trapped water molecules from the cavities of CBn and found that this energy is a maximum for CB7. Moreover, CB7 requires a higher number of water molecules to fill up its cavity. Thus, the expulsion of these high-energy water molecules from the cavity of the CB7 accounts for the entropic gain of this step.[67] Deep penetration of the dye molecule inside the hydrophobic cavity of CB7 causes the release of a large number of cavity water molecules, providing the significant entropic gain in orientational and translational terms. Here, the intricate interplay between the energetic frustration and absolute number of trapped water molecules inside the cavity of CB7 can account for the very high binding constant between 7-DCCA and CB7. In the second step of complex formation, where 1:2 complex formation is taking place, the process is again enthalpy driven ($|H| > |T\Delta S|$). Now, the step is enthalpically favorable but not entropically. This step is highly exothermic although the change of entropy of this step is negative. This negative value of the change of this step is mainly due to the loss of freedom of movement of the dye, which binds with the macrocycle CB7, thereby completing its capsulation. In the case of HP-γ-CD, lack of deep penetration of the dye 7-DCCA inside the cavity causes release of a lesser amount of high-enthalpy trapped water molecules. This type of water molecule, which is different than those in CB7, restores their H-bonding network after release to cause the decrease of entropy. The most important aspect to be mentioned here is that the binding constant values obtained from ITC measurement are significantly different from those obtained from fluorescence measurement. In the case of the 7-DCCA−HP-γ-CD complex, the binding constant values are K_1 = 65 (±37) M^{-1} and K_2 = 6 (±1) M^{-1}, whereas the values obtained from the steady-state fluorescence are 1580 (±620) M^{-1} and 9 (±6) M^{-1}. Again, it is observed that in the case of 7-DCCA−CB7 complex the binding constant values obtained from ITC are significantly different from those

dx.doi.org/10.1021/jp502944h | J. Phys. Chem. B 2014, 118, 9768−9781

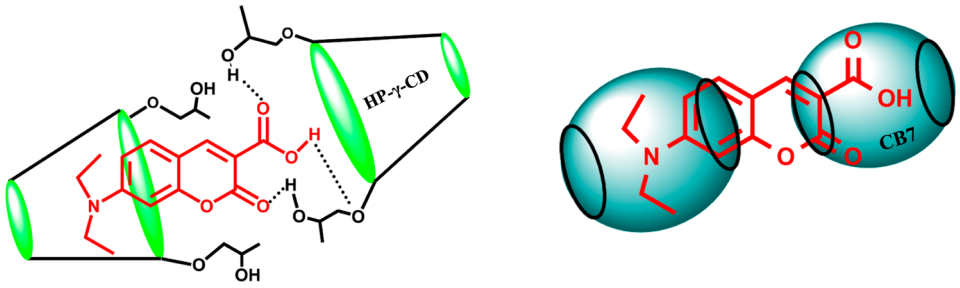

Figure 10. Schematic representation of structure of complexes between 7-DCCA and HP-γ-CD and CB7.

obtained from fluorescence measurement. The binding constant values, which we obtain from ITC experiment, are the binding constant values for the ground-state interaction between the host and guest molecules. On the other hand, the binding constant values obtained from fluorescence measurement indicate the nature and strength of interaction between the host and guest molecule in the excited state of the guest molecule. The binding constant values and enthalpy changes obtained from the fluorescence measurement and ITC measurements are same if the binding reaction is a two-state transition between free and bound molecules by following a lock and key or rigid body mechanism and if the spectroscopic signal change reflects the total population of free and bound molecules.[68] Additionally, these two binding constant values may be the same if there is no change in the hydration state of the interface.[68] In the case of the 7-DCCA−HP-γ-CD complex, H-bond formation takes place, as is evident from FTIR spectra. After the excitation, the guest molecule becomes more polar; therefore, H-bonding interaction between 7-DCCA and HP-γ-CD becomes stronger. Therefore, the binding constant for the 1:1 complex formation between 7-DCCA and HP-γ-CD increases in the excited state. Similarly, the binding constant of the 1:2 complex formation also increases slightly in the excited state.[64] In the case of the 7-DCCA−CB7 complex, the binding constant values are also significantly different in ground and excited states. We have observed that the value of K_1 in the ground state is higher than that in excited state. The first step of complex formation takes place through the hydrophobic interaction, in which the high-energy water molecules are expelled from the cavity of the CB7. Therefore, after excitation, when the polarity of the dye increases, the hydrophobic interaction becomes weak. This causes the decrease of the 1:1 (guest:host) binding constant K_1 on going from the ground state to the excited state. The 1:2 (guest:host) binding constant K_2 signifies the van der Waals type of interaction between the dye and the macrocycle. After excitation, the electronic distribution within the guest molecule changes to make it more polar than ground state and the extent of van der Waals interaction increases. This causes the increase of the value of K_2.

On the basis of the studies carried out in this work by using different spectroscopic methods (steady-state absorption and emission spectroscopy, time-resolved emission spectroscopy, ^{1}H NMR, FTIR spectroscopy) and isothermal titration calorimetry technique, the probable structures of host−guest complexes between 7-DCCA with HP-γ-CD and CB7 are shown in Figure 10.

3.9. Time-Resolved Anisotropy Measurements. We have studied the time-resolved anisotropy measurement to understand how the host−guest complexation affects the rotational relaxation of the dye. In water, the rotational relaxation time of 7-DCCA is ~90 ps.[46] After addition of 6.93 mM HP-γ-CD, the average rotational relaxation time increases to 645 ps with a fast component of 55 ps (32%) and a slow component of 920 ps (68%) (Table 4 and Figure 11). On the other hand, in the presence of CB7 (2.00×10^{-5} M), the average rotational relaxation time of 7-DCCA rises to 400 ps with a fast component of 130 ps (10%) and a slow component of 430 ps (90%) (Table 4 and Figure 11). In both cases the slow components arise because of the complex formation between the dye and the macrocycles. In a previous study, we showed that in the presence of 12.9 mM γ-CD, 7-DCCA exhibited average rotational relaxation time of 290 ps.[46] Moreover, in the presence of 12.9 mM γ-CD, the two components of average rotational relaxation time are a fast component of 95 ps (40%) and a slow component of 420 ps (60%).[46] We have found that both the 1:1 and 1:2 binding interactions between the dye 7-DCCA and HP-γ-CD are much weaker than that between 7-DCCA and γ-CD. With γ-CD, the binding interaction between 7-DCCA and HP-γ-CD is of a 1:2 nature. Moreover, 1:2 complexations with HP-γ-CD increase

Table 4. Rotational Relaxation Time of 7-DCCA in HP-γ-CD and CB7

sr no.	system	r_0	τ_1 (ns)	a_1	τ_2 (ns)	a_2	$\langle\tau_{rot}\rangle^a$ (ns)
1	7-DCCA in CB7	0.315	0.130	0.100	0.430	0.900	0.400
2	7-DCCA in HP-γ-CD	0.388	0.055	0.316	0.920	0.684	0.645

$^a\langle\tau_{rot}\rangle = a_1\tau_1 + a_2\tau_2$

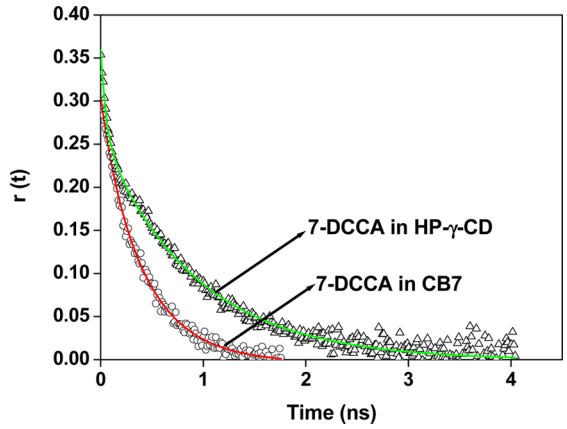

Figure 11. Time-resolved anisotropy decays of 7-DCCA in the presence of HP-γ-CD and CB7.

dx.doi.org/10.1021/jp502944h | J. Phys. Chem. B 2014, 118, 9768−9781

the hydrodynamic volume of the complex up to such an extent that overall rotational relaxation time of the system (7-DCCA–HP-γ-CD complex) increases ∼2.2 times from that of host–guest complex with γ-CD. In both cases the slow component is due to the dye–macrocycle complexes. To get an idea about the size of the dye-macrocycles complexes, we have used the following relation:[69]

$$\tau_2 = \frac{4\pi\eta r_h^3}{3kT} \quad (7)$$

where r_h is the hydrodynamic radius of the dye–macrocycle complexes, η the viscosity of the medium, and k the Boltzmann constant; T is 298 K. We have used the time constants of the slower component of the anisotropy decay (τ_2) to estimate the value of r_h. The estimated value of r_h in the case of the 7-DCCA–CB7 complex is 7.5 Å. Therefore, the estimated diameter of the complex is 15 Å. In the case of the 7-DCCA–HP-γ-CD complex, r_h was estimated as 9.7 Å. Therefore, the estimated diameter of the complex is 19.4 Å. Therefore, in both cases of the addition of macrocycles, a dye–macrocycle complex is formed. For this reason, the diameter of the complex is increased compared to that of the free dye.

4. CONCLUSION

The supramolecular host–guest complexation between a hydrophilic dye, 7-DCCA, with two highly water-soluble macrocycles, HP-γ-CD and CB7, has been extensively studied. The fundamental differences in the properties and nature of the cavity on the inclusion phenomenon were discussed in this contribution. The effect of different macrocycles on the photophysics of 7-DCCA was observed. We have found that addition of HP-γ-CD caused blue shifting of the absorption spectra of 7-DCCA in water, whereas addition of CB7 caused the opposite effect. Moreover, blue shift in the emission peak of 7-DCCA after addition of HP-γ-CD demonstrates the complex formation between the dye and HP-γ-CD. The addition of CB7 causes a very small change in the emission peak of 7-DCCA followed by an increase of fluorescence intensity as well as fluorescence quantum yield, demonstrating the formation of a complex. In the case of complex formation between 7-DCCA and HP-γ-CD, H-bonding interaction plays a prominent role. This H-bonding interaction between the dye and HP-γ-CD causes the shallow degree of penetration of the dye inside the cavity of HP-γ-CD. On the other hand, deep penetration of the dye inside the highly hydrophobic cavity of CB7 strongly prevents the TICT state formation. This causes the greater increase of fluorescence quantum yield of 7-DCCA in CB7 compared to that in HP-γ-CD. The binding constant measurement by means of nonlinear curve fitting shows that 7-DCCA formed a 1:2 complex with HP-γ-CD and CB7. We have also performed time-resolved emission measurements for the dye in the presence of both macrocycles and found considerable change in decay times. This shows the formation of host–guest complex, and the nature of the complexes with two macrocycles is different. Significant shift in the bond vibration frequencies in the FTIR studies shows the encapsulation of the dyes in the hydrophobic cavity of the macrocycles. This is further substantiated by the ^{1}H NMR studies in which the upfield and downfield shifts of the protons were observed in both the aliphatic and aromatic region in the presence of macrocycles. An isothermal titration calorimetry study confirms our proposal of 1:2 complex formation between 7-DCCA with both HP-γ-CD and CB7. This also provided the same information about the weaker binding of 7-DCCA with HP-γ-CD compared to that with CB7 as observed from the fluorescence study.

■ ASSOCIATED CONTENT

Supporting Information

Thermodynamic parameters obtained from ITC measurements and the change of (i) absorption spectra, (ii) weight percentage of fluorescence emission decays, (iii) residual of fitting of time-resolved fluorescence emission spectral decays, and (iv) FTIR spectra of 7-DCCA in the presence of macrocyclic hosts. This material is available free of charge via the Internet at http://pubs.acs.org.

■ AUTHOR INFORMATION

Corresponding Author

*E-mail: debabrata@iitp.ac.in. Fax: 91-612-2277383.

Notes

The authors declare no competing financial interest.

■ ACKNOWLEDGMENTS

D.S. thanks IIT Patna, India for research facilities. A.C. thanks CSIR, New Delhi for research fellowship. B.M. is thankful to IIT Patna for research fellowship. Authors are thankful to reviewers for their valuable comments.

■ REFERENCES

(1) Koner, A. L.; Nau, W. M. Cucurbituril Encapsulation of Fluorescent Dyes. *Supramol. Chem.* **2007**, *19*, 55–66.
(2) Bhasikuttan, A. C.; Dutta Choudhury, S.; Pal, H.; Mohanty, J. Supramolecular Assemblies of Thioflavin T with Cucurbiturils: Prospects of Cooperative and Competitive Metal Ion Binding. *Isr. J. Chem.* **2011**, *51*, 634–645.
(3) Chen, Y.; Liu, Y. Cyclodextrin-Based Bioactive Supramolecular Assemblies. *Chem. Soc. Rev.* **2010**, *39*, 495–505.
(4) Arunkumar, E.; Forbes, C. C.; Smith, B. D. Improving the Properties of Organic Dyes by Molecular Encapsulation. *Eur. J. Org. Chem.* **2005**, 4051–4059.
(5) Wagner, B. D. Recent Applications of Host-Guest Inclusion in Fluorescence-Based Trace Analysis. *Curr. Anal. Chem.* **2007**, *3*, 183–195.
(6) Fakayode, S. O.; Lowry, M.; Fletcher, K. A.; Huang, X.; Powe, A. M.; Warner, I. M. Cyclodextrins Host-Guest Chemistry in Analytical and Environmental Chemistry. *Curr. Anal. Chem.* **2007**, *3*, 171–181.
(7) Dsouza, R. N.; Pischel, U.; Nau, W. M. Fluorescent Dyes and Their Supramolecular Host/Guest Complexes with Macrocycles in Aqueous Solution. *Chem. Rev. (Washington, DC, U.S.)* **2011**, *111*, 7941–7980.
(8) Behrend, R.; Meyer, E.; Rusche, F. Ueber Condensationsproducte Aus Glycoluril Und Formaldehyde. *Liebigs Ann. Chem.* **1905**, *339*, 1–37.
(9) Nau, W. M.; Scherman, O. A. The World of Cucurbiturils — From Peculiarity to Commodity. *Isr. J. Chem.* **2011**, *51*, 492–494.
(10) Freeman, W. A.; Mock, W. L.; Shih, N. Y. Cucurbituril. *J. Am. Chem. Soc.* **1981**, *103*, 7367–7368.
(11) Uzunova, V. D.; Cullinane, C.; Brix, K.; Nau, W. M.; Day, A. I. Toxicity of Cucurbit[7]uril and Cucurbit[8]uril: An Exploratory in Vitro and in Vivo Study. *Org. Biomol. Chem.* **2010**, *8*, 2037–2042.
(12) Navajas, P. M.; Corma, A.; Garcia, H. Complexation and Fluorescence of Tricyclic Basic Dyes Encapsulated in Cucurbiturils. *ChemPhysChem* **2008**, *9*, 713–720.
(13) Barooah, N.; Mohanty, J.; Pal, H.; Bhasikuttan, A. C. Stimulus-Responsive Supramolecular pK_a Tuning of Cucurbit[7]uril Encapsulated Coumarin 6 Dye. *J. Phys. Chem. B* **2012**, *116*, 3683–3689.

(14) Freitag, M.; Gundlach, L.; Piotrowiak, P.; Galoppini, E. Fluorescence Enhancement of Di-*p*-tolyl Viologen by Complexation in Cucurbit[7]uril. *J. Am. Chem. Soc.* **2012**, *134*, 3358−3366.
(15) Mohanty, J.; Thakur, N.; Choudhury, S. D.; Barooah, N.; Pal, H.; Bhasikuttan, A. C. Recognition-Mediated Light-Up of Thiazole Orange with Cucurbit[8]uril: Exchange and Release by Chemical Stimuli. *J. Phys. Chem. B* **2012**, *116*, 130−135.
(16) Yi, S.; Captain, B.; Ottaviani, M. F.; Kaifer, A. E. Controlling the Extent of Spin Exchange Coupling in 2,2,6,6-Tetramethylpiperidine-1-oxyl (TEMPO) Biradicalsvia Molecular Recognition with Cucurbit-[*n*]uril Hosts. *Langmuir* **2011**, *27*, 5624−5632.
(17) Shaikh, M.; Mohanty, J.; Singh, P. K.; Nau, W. M.; Pal, H. Complexation of Acridine Orange by Cucurbit[7]uril and *β*-Cyclodextrin: Photophysical Effects and pK_a Shifts. *Photochem. Photobiol. Sci.* **2008**, *7*, 408−414.
(18) Chakraborty, B.; Basu, S. Deciphering the Host−Guest Chemistry of Acridine Yellow and Cucurbit[7]uril: An Integrated Spectroscopic and Calorimetric Study. *Chem. Phys. Lett.* **2011**, *507*, 74−79.
(19) Marquez, C.; Nau, W. M. Polarizabilities Inside Molecular Containers. *Angew. Chem., Int. Ed.* **2001**, *40*, 4387−4390.
(20) Barooah, N.; Mohanty, J.; Pal, H.; Bhasikuttan, A. C. Non-Covalent Interactions of Coumarin Dyes with Cucurbit[7]uril Macrocycle: Modulation of ICT to TICT State Conversion. *Org. Biomol. Chem.* **2012**, *10*, 5055−5062.
(21) Choudhury, S. D.; Mohanty, J.; Pal, H.; Bhasikuttan, A. C. Cooperative Metal Ion Binding to a Cucurbit[7]uril−Thioflavin T Complex: Demonstration of a Stimulus-Responsive Fluorescent Supramolecular Capsule. *J. Am. Chem. Soc.* **2010**, *132*, 1395−1401.
(22) Feng, Y.; Xue, S. F.; Fan, Z. F.; Zhang, Y. Q.; Zhu, Q. J.; Tao, Z. Host−Guest Complexes of Some Cucurbit[*n*]urils with the Hydrochloride Salts of Some Imidazole Derivatives. *J. Inclusion Phenom. Macrocyclic Chem.* **2009**, *64*, 121−131.
(23) Carvalho, C. P.; Uzunova, V. D.; Silva, J. P. D.; Nau, W. M.; Pischel, U. Photoinduced pH Jump Applied to Drug Release from Cucurbit[7]uril. *Chem. Commun (Cambridge, U.K.)* **2011**, *47*, 8793−8795.
(24) Li, C.; Li, J.; Jia, X. Selective Binding and Highly Sensitive Fluorescent Sensor of Palmatine and Dehydrocorydaline Alkaloids by Cucurbit[7]uril. *Org. Biomol. Chem.* **2009**, *7*, 2699−2703.
(25) Gavvala, K.; Sengupta, A.; Koninti, R. K.; Hazra, P. Supramolecular Host-Inhibited Excited-State Proton Transfer and Fluorescence Switching of the Anti-Cancer Drug, Topotecan. *ChemPhysChem* **2013**, *14*, 3375−3383.
(26) Gavvala, K.; Sengupta, A.; Hazra, P. Modulation of Photophysics and pK_a Shift of the Anti-cancer Drug Camptothecin in the Nanocavities of Supramolecular Hosts. *ChemPhysChem* **2013**, *14*, 532−542.
(27) Hassonville, S. H. D.; Perly, B.; Piel, G.; Hees, T. V.; Barillaro, V.; Bertholet, P.; Delattre, L. Inclusion Complexes of Cyproterone Acetate with Cyclodextrins in Aqueous Solution. *J. Inclusion Phenom. Macrocyclic Chem.* **2002**, *44*, 289−292.
(28) Mondal, S. K.; Sahu, K.; Ghosh, S.; Sen, P.; Bhattacharyya, K. Excited-State Proton Transfer from Pyranine to Acetate in *γ*-Cyclodextrin and Hydroxypropyl *γ*-Cyclodextrin. *J. Phys. Chem. A* **2006**, *110*, 13646−13652.
(29) Cigáň, M.; Donovalová, J.; Szöcs, V.; Gašpar, J.; Jakusová, K.; Gáplovský, A. 7-(Dimethylamino)coumarin-3-carbaldehyde and Its Phenylsemicarbazone: TICT Excited State Modulation, Fluorescent H-Aggregates, and Preferential Solvation. *J. Phys. Chem. A* **2013**, *117*, 4870−4883.
(30) Gupta, M.; Maity, D. K.; Singh, M. K.; Nayak, S. K.; Ray, A. K. Supramolecular Interaction of Coumarin 1 Dye with Cucurbit[7]uril as Host: Combined Experimental and Theoretical Study. *J. Phys. Chem. B* **2012**, *116*, 5551−5558.
(31) Hazra, P.; Chakrabarty, D.; Sarkar, N. Intramolecular Charge Transfer and Solvation Dynamics of Coumarin 152 in Aerosol-OT, Water-Solubilizing Reverse Micelles, and Polar Organic Solvent Solubilizing Reverse Micelles. *Langmuir* **2002**, *18*, 7872−7879.
(32) Verma, P.; Pal, H. Intriguing H-Aggregate and H-Dimer Formation of Coumarin-481 Dye in Aqueous Solution As Evidenced from Photophysical Studies. *J. Phys. Chem. A* **2012**, *116*, 4473−4484.
(33) Gustavsson, T.; Cassara, L.; Gulbinas, V.; Gurzadyan, G.; Mialocq, J.-C.; Pommeret, S.; Sorgius, M.; van der Meulen, P. Femtosecond Spectroscopic Study of Relaxation Processes of Three Amino-Substituted Coumarin Dyes in Methanol and Dimethyl Sulfoxide. *J. Phys. Chem. A* **1998**, *102*, 4229−4245.
(34) Das, K.; Jain, B.; Patel, H. S. Hydrogen Bonding Properties of Coumarin 151, 500, and 35: The Effect of Substitution at the 7-Amino Position. *J. Phys. Chem. A* **2006**, *110*, 1698−1704.
(35) Scypinski, S.; Drake, J. M. Photophysics of Coumarin Inclusion Complexes with Cyclodextrin. Evidence for Normal and Inverted Complex Formation. *J. Phys. Chem.* **1985**, *89*, 2432−2435.
(36) Yip, R. W.; Wen, Y.-X.; Szabo, A. G. Decay Associated Fluorescence Spectra of Coumarin 1 and Coumarin 102: Evidence for a Two-State Solvation Kinetics in Organic Solvents. *J. Phys. Chem.* **1993**, *97*, 10458−10462.
(37) Morimoito, A.; Yatsuhashi, T.; Shimada, T.; Biczók, L.; Tryk, D. A.; Inoue, H. Radiationless Deactivation of an Intramolecular Charge Transfer Excited State through Hydrogen Bonding: Effect of Molecular Structure and Hard−Soft Anionic Character in the Excited State. *J. Phys. Chem. A* **2001**, *105*, 10488−10496.
(38) Moog, R. S.; Kim, D. D.; Oberle, J. J.; Ostrowski, S. G. Solvent Effects on Electronic Transitions of Highly Dipolar Dyes: A Comparison of Three Approaches. *J. Phys. Chem. A* **2004**, *108*, 9294−9301.
(39) Chang, T. L.; Cheung, H. C. A Model for Molecules with Twisted Intramolecular Charge Transfer Characteristics: Solvent Polarity Effect on the Nonradiative Rates of Dyes in a Series of Water—Ethanol Mixed Solvents. *Chem. Phys. Lett.* **1990**, *173*, 343−348.
(40) Jones, G., II; Feng, Z.; Bergmark, W. R. Photophysical Properties of (Dimethylamino)anthraquinones: Radiationless Transitions in Solvent and Polyelectrolyte Media. *J. Phys. Chem.* **1994**, *98*, 4511−4516.
(41) Rettig, W.; Koutecký, V. B. On a Possible Mechanism of the Multiple Fluorescence of *p*-N, N-Dimethylaminobenzonitrile and Related Compounds. *Chem. Phys. Lett.* **1979**, *62*, 115−120.
(42) Grabowski, Z. R.; Rotkiewicz, K.; Rettig, W. Structural Changes Accompanying Intramolecular Electron Transfer: Focus on Twisted Intramolecular Charge-Transfer States and Structures. *Chem. Rev. (Washington, DC, U.S.)* **2003**, *103*, 3899−4031.
(43) Ramakrishna, G.; Ghosh, H. N. Efficient Electron Injection from Twisted Intramolecular Charge Transfer (TICT) State of 7-Diethyl amino coumarin 3-carboxylic Acid (D-1421) Dye to TiO_2 Nanoparticle. *J. Phys. Chem. A* **2002**, *106*, 2545−2553.
(44) Zhang, H.; Yu, T.; Zhao, Y.; Fan, D.; Chen, L.; Qiu, Y.; Qian, L.; Zhang, K.; Yang, C. Crystal Structure and Photoluminescence of 7-(*N*,*N*′-Diethylamino)-coumarin-3-carboxylic Acid. *Spectrochim. Acta, Part A* **2008**, *69*, 1136−1139.
(45) Tablet, C.; Matei, I.; Pincu, E.; Meltzer, V.; Hillebrand, M. Spectroscopic and Thermodynamic Studies of 7-Diethylamino-coumarin-3-carboxylic Acid in Interaction with *β*- and 2-Hydroxypropyl-*β*-cyclodextrins. *J. Mol. Liq.* **2012**, *168*, 47−53.
(46) Chatterjee, A.; Seth, D. Photophysical Properties of 7-(Diethylamino)coumarin-3-carboxylic Acid in the Nanocage of Cyclodextrins and in Different Solvents and Solvent Mixtures. *Photochem. Photobiol.* **2013**, *89*, 280−293.
(47) Chatterjee, A.; Maity, B.; Seth, D. The Photophysics of 7-(*N*,*N*′-Diethylamino)coumarin-3-carboxylic Acid in Water/AOT/Isooctane Reverse Micelles: An Excitation Wavelength Dependent Study. *Phys. Chem. Chem. Phys.* **2013**, *15*, 1894−1906.
(48) Chatterjee, A.; Maity, B.; Seth, D. Influence of Double Confinement on Photophysics of 7-(Diethylamino)coumarin-3-carboxylic Acid in Water/AOT/Isooctane Reverse Micelles. *RSC Adv.* **2014**, *4*, 13989−14000.
(49) Jones, G., II; Jackson, W. R.; Choi, C. Y.; Bergmark, W. R. Solvent Effects on Emission Yield and Lifetime for Coumarin Laser

Dyes. Requirements for a Rotatory Decay Mechanism. *J. Phys. Chem.* **1985**, *89*, 294−300.
(50) Steed, J.W.; Atwood, J.L. *Supramolecular Chemistry*, 2nd ed.; John Wiley & Sons, Ltd: Chichester, U.K., 2009; p 325.
(51) Edwards, J. Molecular Volumes and the Stokes−Einstein Equation. *J. Chem. Educ.* **1970**, *47*, 261−270.
(52) Nau, W. M.; Mohanty, J. Taming Fluorescent Dyes with Cucurbituril. *Int. J. Photoenergy* **2005**, *7*, 133−141.
(53) Wagner, B. D. Hydrogen Bonding of Excited States in Supramolecular Host−Guest Inclusion Complexes. *Phys. Chem. Chem. Phys.* **2012**, *14*, 8825−8835.
(54) Velasco, J.; Guardado, P.; Carmona, C.; Munoz, M. A.; Balon, M. Guest−Host Interactions Between Tetrahydrobetacarboline and β-cyclodextrin. *J. Chem. Soc., Faraday Trans.* **1998**, *94*, 1469−1476.
(55) Nigam, S.; Durocher, G. Spectral and Photophysical Studies of Inclusion Complexes of Some Neutral 3H-Indoles and Their Cations and Anions with β-Cyclodextrin. *J. Phys. Chem.* **1996**, *100*, 7135−7142.
(56) Martin, C.; Cohen, B.; Gaamoussi, I.; Ijjaali, M.; Douhal, A. Ultrafast Dynamics of C30 in Solution and within CDs and HSA Protein. *J. Phys. Chem. B* **2014**, *118*, 5760−5771.
(57) Wagner, B. D. The Use of Coumarins as Environmentally-Sensitive Fluorescent Probes of Heterogeneous Inclusion Systems. *Molecules* **2009**, *14*, 210−237.
(58) Zhang, X.; Gramlich, G.; Wang, X.; Nau, W. M. A Joint Structural, Kinetic, and Thermodynamic Investigation of Substituent Effects on Host−Guest Complexation of Bicyclic Azoalkanes by β-Cyclodextrin. *J. Am. Chem. Soc.* **2002**, *124*, 254−263.
(59) Sambasevam, K. P.; Mohamad, S.; Sarih, N. M.; Ismail, N. A. Synthesis and Characterization of the Inclusion Complex of β-Cyclodextrin and Azomethine. *Int. J. Mol. Sci.* **2013**, *14*, 3671−3682.
(60) Zhou, C.; Cheng, X.; Zhao, Q.; Yan, Y.; Wang, J.; Huang, J. Self-Assembly of Nonionic Surfactant Tween 20@2β-CD Inclusion Complexes in Dilute Solution. *Langmuir* **2013**, *29*, 13175−13182.
(61) Huang, C. Y. [27] Determination of Binding Stoichiometry by the Continuous Variation Method: The Job Plot. *Methods Enzymol.* **1982**, *87*, 509−525.
(62) Ross, P. D.; Subramanian, S. Thermodynamics of Protein Association Reactions: Forces Contributing to Stability. *Biochemistry* **1981**, *20*, 3096−3−102.
(63) Liao, D.; Dai, S.; Tam, K. C. Interaction Between Fluorocarbon End-Capped Poly(ethylene oxide) and Cyclodextrins. *Macromolecules* **2007**, *40*, 2936−2945.
(64) Nilsson, M.; Valente, A. J. M.; Olofsson, G.; Söderman, O.; Bonini, M. Thermodynamic and Kinetic Characterization of Host−Guest Association between Bolaform Surfactants and α- and β-Cyclodextrins. *J. Phys. Chem. B* **2008**, *112*, 11310−11316.
(65) Kano, K.; Nishiyabu, R.; Doi, R. Novel Behavior of *O*-Methylated β-Cyclodextrins in Inclusion of *meso*-Tetraarylporphyrins. *J. Org. Chem.* **2005**, *70*, 3667−3673.
(66) Miyake, K.; Yasuda, S.; Harada, A.; Sumaoka, J.; Komiyama, M.; Shigekawa, H. Formation Process of Cyclodextrin Necklace−Analysis of Hydrogen Bonding on a Molecular Level. *J. Am. Chem. Soc.* **2003**, *125*, 5080−5085.
(67) Biedermann, F.; Uzunova, V. D.; Scherman, O. A.; Nau, W. M.; De Simone, A. Release of High-Energy Water as an Essential Driving Force for the High-Affinity Binding of Cucurbit[*n*]urils. *J. Am. Chem. Soc.* **2012**, *134*, 15318−15323.
(68) Jelesarov, I.; Bosshard, H. R. Isothermal Titration Calorimetry and Differential Scanning Calorimetry as Complementary Tools to Investigate the Energetics of Biomolecular Recognition. *J. Mol. Recognit.* **1999**, *12*, 3−18.
(69) Sen, P.; Roy, D.; Mondal, S. K.; Sahu, K.; Ghosh, S.; Bhattacharyya, K. Fluorescence Anisotropy Decay and Solvation Dynamics in a Nanocavity: Coumarin 153 in Methyl β-Cyclodextrins. *J. Phys. Chem. A* **2005**, *109*, 9716−9722.